

Electro-Induced Dewetting and Concomitant Ionic Current Avalanche in Nanopores

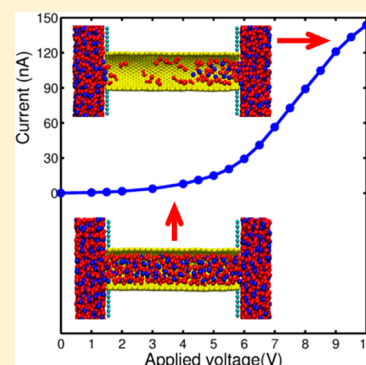
Xikai Jiang,[†] Jingsong Huang,[‡] Bobby G. Sumpter,[‡] and Rui Qiao^{*,†}

[†]College of Engineering & Science, Clemson University, 237 Fluor Daniel Building, Clemson, South Carolina 29634-0921, United States

[‡]Center for Nanophase Materials Sciences and Computer Science & Mathematics Division, Oak Ridge National Laboratory, Bethel Valley Road, Oak Ridge, Tennessee 37831-6367, United States

Supporting Information

ABSTRACT: Electrically driven ionic transport of room-temperature ionic liquids (RTILs) through nanopores is studied using atomistic simulations. The results show that in nanopores wetted by RTILs a gradual *dewetting* transition occurs upon increasing the applied voltage, which is accompanied by a sharp *increase* in ionic current. These phenomena originate from the solvent-free nature of RTILs and are in stark contrast with the transport of conventional electrolytes through nanopores. Amplification is possible by controlling the properties of the nanopore and RTILs, and we show that it is especially pronounced in charged nanopores. The results highlight the unique physics of nonequilibrium transport of RTILs in confined geometries and point to potential experimental approaches for manipulating ionic transport in nanopores, which can benefit diverse techniques including nanofluidic circuitry and nanopore analytics.



SECTION: Physical Processes in Nanomaterials and Nanostructures

Ionic transport in nanopores plays a crucial role in a number of important technologies, ranging from nanopore DNA sequencing for biological/medical research to nanoporous carbon supercapacitors for energy storage.^{1,2} Many intriguing phenomena have been discovered for ionic transport on the nanoscale,^{3–9} including rich nonlinear behavior such as current rectification in charged conical nanopores.^{6,9,10} It has also been predicted that in narrow hydrophobic pores that are initially unwetted by aqueous electrolytes an abrupt wetting transition can be triggered by the application of strong electric fields that will consequently cause ionic current jumps from zero to a finite value.^{11,12} This theoretical prediction has recently been experimentally demonstrated.¹³ These unusual phenomena have been extensively studied, and the underlying mechanisms are now understood reasonably well.^{7,14,15} A key finding is that the macroscopic behavior of ionic transport through nanopores, often characterized by a current–voltage (I – V) curve, strongly depends on the thermodynamic states of the ions such as ion concentration and solvation in nanopores. Whereas thermodynamic states of ions in nanopores are typically controlled by the properties of pore walls such as charge density and wetting behavior, they can also be modulated by applied electric fields if the nanopore–electrolyte systems (e.g., charged conical pores immersed in dilute electrolytes) are driven far from equilibrium by the applied field.

Most prior research on ionic transport in nanopores is limited to nanopores connected to aqueous electrolyte reservoirs. Ionic transport in nanopores filled with nonaqueous

electrolytes has received much less attention despite the fact that nonaqueous electrolytes are widely used in electrochemical systems, whose performance is often controlled by their transport in nanopores. We are interested in ionic transport in nanopores filled with room-temperature ionic liquids (RTILs), which are composed exclusively of ions that remain liquid at room-temperature.¹⁶ Because of their wide electrochemical window, low vapor pressure, and nonflammability, RTILs have emerged as a good candidate for electrolytes in many electrochemical systems.^{16–19} Prior research on the ionic transport of RTILs in nanopores focused primarily on the self-diffusion of the ions, revealing that diffusion can be hindered or enhanced compared with that in bulk RTILs depending on the size of nanopore and the molecular structure of ions.^{20–23} However, research on nonequilibrium transport of RTILs is far more limited. The seminal paper by the Siwy group reported current rectification observed in conical nanopores with a narrow-end diameter of 5–7 nm.²⁴ Nonequilibrium transport of RTILs in smaller pores with size comparable to the ion size remains to be systematically investigated.

Here we use atomistic molecular dynamics (MD) simulations to study the ionic transport of RTILs through a nanopore driven by an electric field. Figure 1 shows a schematic of the simulated system, which consists of a nanopore with two

Received: July 20, 2013

Accepted: August 29, 2013

Published: August 29, 2013

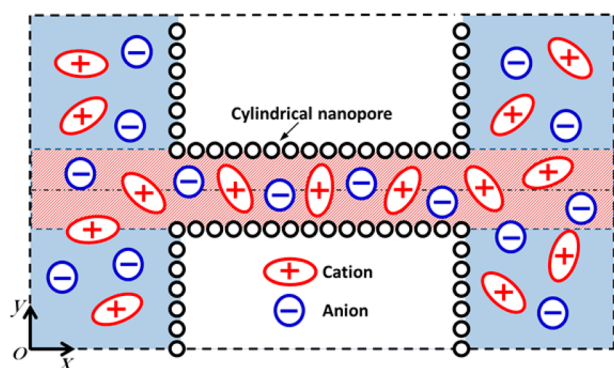


Figure 1. Schematic of the MD system for studying ionic transport of RTILs through a nanopore driven by electric fields. The system consists of a nanopore and an RTIL reservoir. Dashed lines denote the periodic simulation box, which measures 20.0, 12.3, and 12.3 nm in x , y , and z directions, respectively.

ends connected to a reservoir filled with [BMIM][PF₆], an imidazolium-based RTIL. A (32, 0) single-wall carbon nanotube with a center-to-center diameter of 2.51 nm was used as the nanopore. Taking a diameter of 0.34 nm for the carbon atoms, the access diameter of the nanopore is 2.17 nm. Hereafter, the access diameter is used to compute the average RTIL density and conductivity in nanopore. Carbon nanotubes were used as nanopores due to their well-defined geometry. We verified that the phenomena reported here can be reproduced in other nanopores (e.g., those obtained by drilling through a FCC lattice). Two types of nanotubes were studied: neutral nanotubes and charged nanotubes. For charged nanotubes, partial charges of small magnitude were decorated on the pore surface to give a net charge density of -0.05 C/m². The uniform surface charge is similar to that induced by applying a gate voltage to dielectric materials.²⁵ We also studied charged nanotubes in which discrete charge groups were decorated on their surface, and qualitatively similar results were obtained. Two vertical walls, each consisting of carbon atoms arranged in a square lattice (atom spacing is 0.3 nm) were used as boundaries of RTIL reservoir to block the RTIL, allowing it to transport only through the nanopore from one reservoir to the other. To drive ionic transport, we imposed a voltage drop ϕ across the system by applying a uniform electric field along the pore axis (x direction) following $E_x = \phi/L_x$, where L_x is the length of simulation box in the x direction. This method has been validated in the studies of ionic transport through various nanopores.^{10,26} Note that although the applied electric field is uniform, the electrical potential inside the system conforms to the electrostatic law due to a generation of reaction electric fields.^{26,27} The net electrical potential of the ions in the system is the sum of the potential associated with the uniform applied field and the potential due to the reaction electric field. For a given voltage applied across the system, most of the electrical potential drop occurs within the nanopore; consequently, the net electric forces are much larger for ions inside the nanopores than for ions in the reservoir (Figure S1, Supporting Information). Note that at zero applied voltage drop the nanopores are wetted by RTILs, and this is consistent with the fact that the RTILs studied here can wet nanopores with even smaller diameter (~ 0.9 nm).^{19,28,29}

Figure 2a shows the I – V curve in the neutral nanopore. For applied voltages $\phi < 2$ V, the ionic current increases nearly linearly with increasing applied voltage and the effective

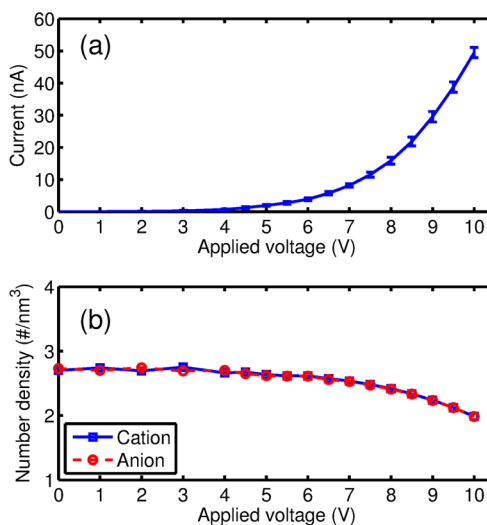


Figure 2. Variation of the ionic current (a) and average ion number density in the central portion of the nanopore (b) as a function of the voltage drop across the entire system. The nanopore surface is electrically neutral.

nanopore conductance is small. At higher voltages, the I – V curve becomes highly nonlinear and the effective nanopore conductance increases sharply. This latter observation is unusual because nonlinear I – V curves and greater effective conductance at higher applied voltages have been observed in nanopores but typically only in charged conical nanopores^{6,9} rather than in the neutral and cylindrical nanopore studied here. Another interesting aspect of the ionic transport is that as the applied voltage increases the density of RTILs inside the nanopore reduces. As shown in Figure 2b, for applied voltages $\phi < 6$ V, the ion density in the central portion of the nanopore (defined here as within 1.0 nm from the middle plane of the nanopore, i.e., $x = 9$ – 11 nm in Figure 1) initially changes little but reduces notably as ϕ increases. At $\phi = 10$ V, the ion density inside the pore is $\sim 75\%$ of that at $\phi = 0$ V.

These unusual phenomena originate from the fact that for RTILs confined in nanopores, under strong electric fields, the ionic conductivity is larger than that of bulk RTILs, and it increases with decreasing ion density. To validate this point, we first performed a series of simulations to compute the ionic conductivity of RTILs confined in nanopores with the same size as that previously considered but periodic along the pore axis. In these simulations, different numbers of RTIL molecules were placed inside the nanopore so that the average ion density varied from 100 to 80% of that found in Figure 2b at zero voltage ($\rho_{\text{ion},\phi=0}$), that is, from 2.68 to 2.14 #/nm³. The method for computing the conductivity of RTILs in a periodic nanopore, together with that for bulk RTILs, can be found in the Supporting Information. Figure 3 shows that with the same average ion density the conductivity of RTILs increases as the electric field E becomes stronger. In fact, when the ion density inside nanopore is the same as $\rho_{\text{ion},\phi=0}$, the conductivity of RTILs confined in the nanopore is smaller than that of bulk RTILs at $E = 0.1$ V/nm, but it exceeds the latter when $E > 0.8$ V/nm. Note that the comparison is made between the conductivity of the ions in nanopore at 0.8 V/nm and that of ions in the bulk at 0.1 V/nm due to the negligible voltage drop in the bulk (Figure S1, Supporting Information). These behaviors are consistent with the results on the ionic transport of RTILs previously reported. In particular, the weaker

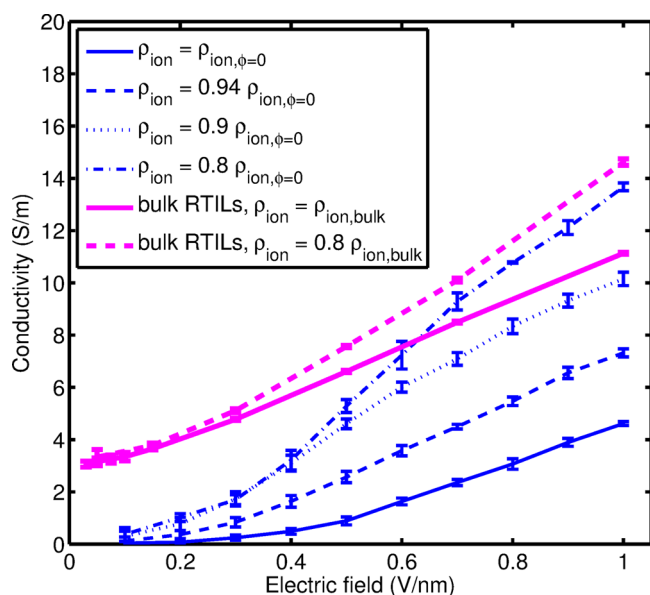


Figure 3. Conductivity of bulk RTILs and RTILs confined in neutral and periodic nanopores as a function of ion density and strength of electric fields.

conductivity of RTILs in the nanopore at low electric fields compared with that in the bulk is in line with the slower self-diffusion of RTILs in nanopore previously reported by the Hung group;^{20,22} the increase in conductivity as E increases is similar to that observed for bulk RTILs.³⁰ Figure 3 also shows that the conductivity of RTILs increases sharply when the ion density decreases slightly, indicating that the mobility of ions increases greatly with decreasing ion density. This behavior is in marked contrast with that of aqueous electrolytes, in which the mobility of ions increases only slightly as the density decreases. This difference is caused by the solvent-free nature of RTILs. RTILs are dense liquids in which electrical migration of ions is retarded primarily by ion–ion friction originating from the close ion–ion contacts and is facilitated by a transient atomistic cavity within the liquids. As such, the ion mobility increases greatly as the ion density decreases and diverges as the ion density approaches zero. However, in aqueous electrolytes, the migration of ions is retarded by the surrounding solvent molecules, and the ionic cloud around each ion plays a secondary role.

To understand how the dependence of RTIL's electrical conductivity on the strength of electric fields and ion density revealed in Figure 3 leads to a decrease in ion occupancy in nanopore as electric field strength increases and the nonlinear I – V curve shown in Figure 2, we examined the response of a nanopore/RTIL system (cf. Figure 1) as a voltage drop is impulsively applied across the system (see Figure 4). Once a voltage drop is applied, an electric field is established inside the nanopore. Because the diameter of the nanopore is much smaller than the lateral size of RTIL reservoir and the system is electrically neutral everywhere, most of the potential drop occurs within the nanopore. When a sufficiently large voltage drop is imposed the electric field inside the nanopore can be strong enough that the ionic conductivity of the RTILs in the nanopore exceeds that of bulk RTILs. For example, immediately after a potential difference of 8 V is imposed across the system an electric field of ~ 0.8 V/nm is established inside the nanopore, and the ionic conductivity of RTILs

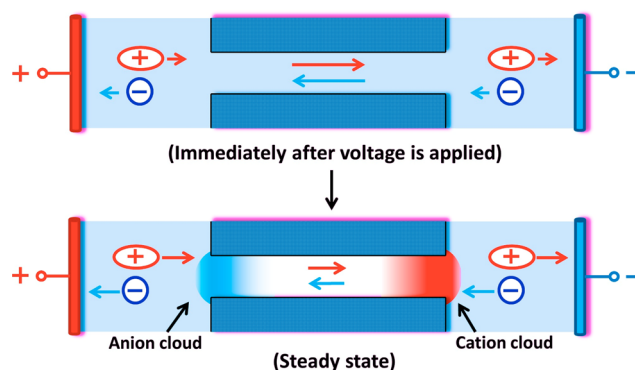


Figure 4. Schematic illustrating the mechanism of ion density reduction in a nanopore filled with an RTIL under large applied voltages. The length of arrows indicates the magnitude of ion flux. The formation of charged ionic clouds near pore entrances (red/blue color denotes ionic cloud with positive/negative charges) and the significant increase in RTIL conductivity as ion density decreases are the main reasons for the reduction of ion density in nanopores under strong applied electric fields.

confined inside the nanopore exceeds that of bulk RTILs (cf. Figure 3). Because of the different ionic conductivities in the nanopore and in the bulk RTILs, the ionic flux inside the nanopore (in Figure 4a, toward the negative electrode for cations and the opposite direction for anions) will be larger than that inside the bulk RTILs. Consequently, cations (anions) start to accumulate near the pore entrance closer to the negative (positive) electrode to form a cation (anion)-rich zone; meanwhile, the number of ions inside the nanopore decreases (cf. Figure 4b). The cation (anion)-rich zone will be termed cationic (anionic) cloud hereafter. Because the number of ions inside the nanopore decreases during this process, the ionic conductivity inside the pore increases (cf. Figure 3), which further enhances the ionic flux through the nanopore, prompting further growth of ionic clouds near the pore entrances. The formation of ionic clouds near the pore entrances creates an electric field within the nanopore that counteracts the electric field initially established due to the imposed voltage drop. As a result, the strength of the net electric field in the nanopore decreases, which tends to reduce the ionic flux through the nanopore and to impede the growth of ionic clouds near the pore entrances. These two effects compete with each other until a steady state of ionic transport through the nanopore is established. At steady state, the ion density inside the nanopore will be smaller than its initial value, and stationary ionic clouds are established near the pore entrances. To quantify the charge accumulation in the ionic clouds near the pore entrances, we computed the ionic charge density in the shaded region shown in Figure 1 at the steady state for an applied potential drop of 10 V. Figure 5 shows that within the nanopore ionic charge density becomes more positive (negative) as we move toward the pore entrance facing the negative (positive) electrode, thus supporting the accumulation of ionic clouds near the pore entrances suggested above. Within the RTIL reservoir, ionic charge density shows strong oscillations near the pore entrances, consistent with the alternating layering of cation/anions observed ubiquitously for interfacial RTILs.^{22,23} The degree of ion depletion inside the pore and the buildup of ionic clouds near the pore entrances at steady state increase rapidly as the applied voltage drop increases. This is because at higher applied voltages,

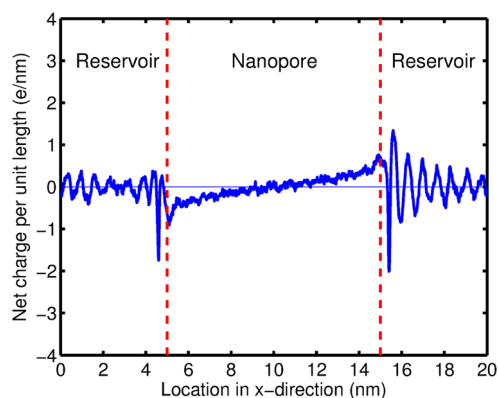


Figure 5. Distribution of ionic space-charge density along the nanopore axis in the shaded region shown in Figure 1. The charge density of nanopore surface is zero. The applied voltage across the nanopore/RTIL reservoir system is 10 V. Distributions of cation and anion density along nanopore axis are shown in Figure S3 in the Supporting Information.

immediately after the voltage is applied, the ionic conductivity inside the nanopore is higher, making the ionic current through the nanopore stronger and consequently the ion depletion and the buildup of ionic clouds more significant. This explains how the dependence of RTIL's electrical conductivity on the strength of electric fields and ion density presented in Figure 3 leads to the decrease in ion occupancy in the nanopore as the applied voltage increases (Figure 2b).

To understand the sharp increase in ionic current as applied voltage ϕ increases (cf. Figure 2a), one can directly analyze the potential drop and ionic conductivity inside nanopore as ϕ increases. However this is not straightforward because the potential drop inside nanopore may not increase monotonically as ϕ increases. This is because as ϕ increases more ions accumulate inside the ionic clouds near pore entrances and they

screen electric fields inside nanopore more significantly, thus lowering the potential drop inside nanopore. Here we adopt a different method, that is, we analyze how the ionic current from RTIL reservoir to nanopore changes as the applied voltage increases. This method is based on the fact that the steady-state ionic current through nanopore is equal to that from the RTIL reservoir to the nanopore, which is governed by the potential drop in RTIL reservoir and the ionic conductivity of bulk RTILs. The potential drop in RTIL reservoir is affected by two factors: the applied voltage across the entire nanopore/RTIL reservoir system and, more importantly, the formation of ionic clouds near the pore entrances. Specifically, charges accumulated in the ionic clouds near pore entrances help increase the potential drop inside the RTIL reservoirs. As pointed out above, when the voltage imposed across the entire nanopore/RTIL reservoir system increases, charge accumulation within each ionic cloud near the pore entrance increases sharply. Therefore, as the applied voltage across the system increases, the increase in potential drop inside RTIL reservoir is faster than the increase in potential drop across the entire system, and this in turn leads to the sharp increase in ionic current through the RTIL reservoir. Equivalently, the ionic current in the entire system increases sharply with the applied voltage, as shown in Figure 2a.

The above discussions suggest that ion depletion in the nanopore and the concomitant sharp increase of ionic current at large voltages are triggered by the high conductivity of RTILs in the nanopore at large voltages and sustained by the increase in ionic conductivity as the ions density decreases. On the basis of these results, we expect that if the conductivity of the RTILs inside nanopore can be increased and the sharp increase in ionic conductivity as ion density reduces can be achieved, then large ionic current through nanopores can be induced and ion depletion can be amplified at lower voltages. Such a situation can, in principle, be achieved by tailoring the surface and geometrical properties of nanopores and the size/shape of

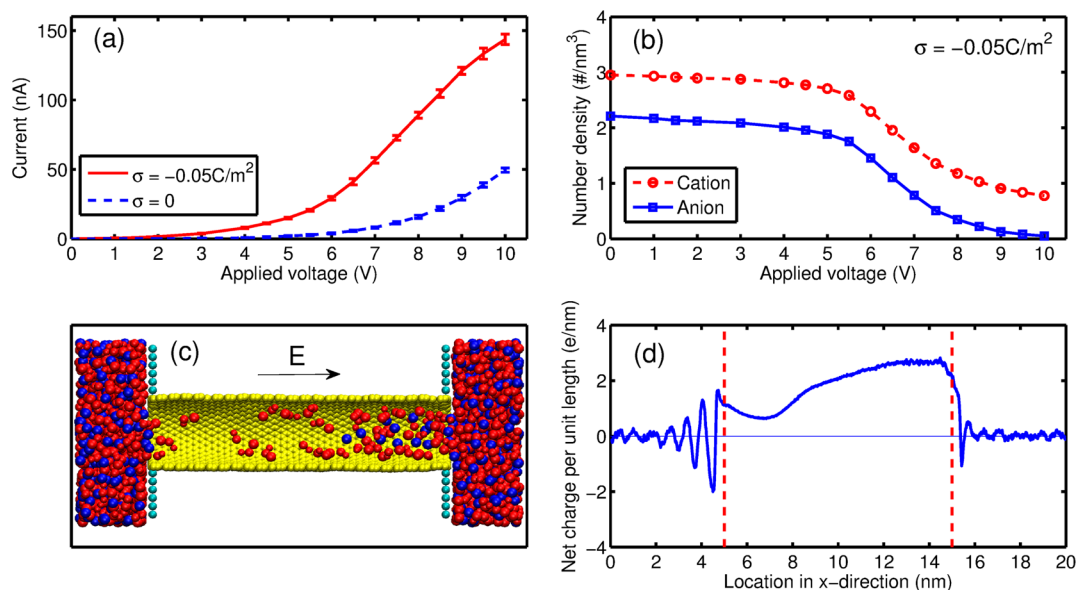


Figure 6. (a) I - V relations in charged nanopores ($\sigma = -0.05\text{C/m}^2$) connected with RTIL reservoirs. (b) Variation of ion density in the central portion of charged nanopore ($9\text{ nm} < x < 11\text{ nm}$) as a function of the applied voltage across the nanopore/RTIL reservoir system. (c) Snapshot of the MD system at an applied voltage of 10 V. Yellow (cyan) balls denote nanopore (vertical wall) atoms. Red (blue) balls denote cations (anions). (d) Distribution of ionic space-charge density at an applied voltage of 10 V along nanopore axis in the shaded region shown in Figure 1. Distributions of cation and anion density along nanopore axis are shown in Figure S4 in the Supporting Information.

RTIL molecules. In particular, such a situation may be achieved in charged nanopores. In charged nanopores, the density of counterions exceeds that of co-ions. Under the action of applied electric fields, the net ionic current is a sum of the migration current due to electrical migration of individual ions and the convective current due to the collective movement of all ions (termed the electroosmotic flow). In narrow nanopores with moderate/high surface charge densities or a smooth surface, the convection current can be much greater than the migration current.^{31,32} For the charged nanopore considered here ($\sigma = -0.05 \text{ C/m}^2$, $D = 2.17 \text{ nm}$), the ionic conductivity of RTILs inside an isolated nanopore (i.e., the nanopore is periodic along its axis and is not connected with an external RTIL reservoir) is 733 S/m at an applied electric field strength of only 0.001 V/nm , and the convection current contributes to $\sim 99.9\%$ of the total ionic conductivity. Figure 6a shows the I - V relation for the RTIL going through this charged nanopore when it is connected to a RTIL reservoir. The I - V curve shows essentially the same feature as that in neutral nanopores, that is, ionic current increases nonlinearly as applied voltage increases, although the magnitude of ionic current is much larger than that in neutral nanopores at any given voltage. Figure 6b shows that at a zero applied voltage more cations (counterions) reside inside the negatively charged nanopore than anions (co-ions). The net charge of ions inside the nanopore is found to balance the charge on the nanopore surface. As the applied voltage increases, the density of both cations and anions in the central portion of the nanopore decreases, but their difference remains nearly the same, which still balances the surface charge on the pore wall. An interesting observation is that at an applied voltage of $\phi = 10 \text{ V}$ anion's density in the central portion of the nanopore drops to nearly zero and the cation's density is reduced to $\sim 30\%$ of that at $\phi = 0 \text{ V}$, which represents a much stronger ion depletion compared with that in neutral nanopores. The decrease in ion density signifies a gradual dewetting transition inside nanopore as the applied voltage increases. Figure 6c shows a snapshot of the MD system at $\phi = 10 \text{ V}$, and it can be clearly seen that a significant portion of nanopore becomes dewetted. The larger ionic current and stronger ion depletion of ions in charged nanopores compared with neutral nanopores are consistent with our expectations. These phenomena have the same physical origins with similar, albeit less pronounced behavior, as observed in neutral nanopores (cf. Figure 2). For example, as shown in Figure 6d, while the ionic space-charge density is nonzero everywhere along the pore axis (due to the presence of net surface charge), the space-charge density near the pore entrance adjacent to the negative electrode is more positive than that near the pore entrance adjacent to the positive electrode. This confirms the formation of ionic clouds near the pore entrances, which was also observed in neutral nanopores. It is worth noting that the onset voltage drop for observing strongly nonlinear I - V curves in both neutral and charged nanopores is smaller than 6 V . Because such onset voltage is comparable to the electrochemical window of RTILs, it helps the experimental realization of the nonlinear phenomena observed here.

In summary, electric-field-driven ionic transport of RTILs through nanopores was studied using atomistic simulations. As the applied voltage increases, the ionic current through the nanopore increases sharply while the ion density inside the nanopore decreases. These unusual phenomena are synergistic results of the unique property of RTILs (ionic conductivity

increases as ion density decreases, which originates from the solvent-free nature of RTILs and the fundamental role of ion-ion friction in controlling electrical ion migration in RTILs) and the far-from equilibrium operation of ionic transport explored here (e.g., formation of stable ionic clouds near the pore entrances under large applied voltages). As a proof-of-concept, we only explored the manipulation of these phenomena by tailoring the surface charge of the nanopores. However, manipulating these phenomena by tailoring other properties of nanopores and RTIL molecules can also be a good strategy. In particular, it should be possible to amplify these phenomena through careful selection of nanopores or RTIL molecules with size/shape optimized for a given nanopore. These strategies will benefit from the recent progress in fabricating nanopores with different sizes and surface functionalization and from the vast diversity of RTILs that potentially can be synthesized. Examining these strategies will help guide rational selection of nanopores and RTILs to harness these phenomena in practical applications.

The highly nonlinear ionic transport of RTILs through nanopores shown here and its variants (e.g., ionic transport through nanopores with discontinuous surface charge densities⁴) can be implemented in solid-state nanopores for applications such as nanofluidic circuitry⁴ and nanopore analytics.⁹ In particular, it could provide new ways of improving sensing and detection of molecules using nanopores. Specifically, in nanopore-based sensing, the passage of molecules through a nanopore causes changes in ionic current or other measurable electrical quantities, and such a change is used for molecular sensing. Present nanopore analytics based on aqueous electrolytes work best for charged and hydrophilic molecules or nanoparticles but face considerable challenges when hydrophobic molecules, which have limited stability in aqueous electrolytes, must be analyzed. Recent experiments demonstrated that molecules with different levels of hydrophobicity can be solvated using RTILs.³³ Such solvation capability of RTILs, along with the other unique advantages of RTILs such as nonvolatility, helps expand the applicability of nanopore analytics to broader classes of molecules and to enhance the performance.

METHODS

MD simulations were performed in the NVT ensemble using the Gromacs package.³⁴ The length of the nanopore and the RTIL reservoir were both 10 nm . Periodic boundary conditions were applied in all three directions. The RTILs were modeled using the force field developed in ref 35, and the carbon nanotube was modeled using the force field described in ref 36. The vertical walls were modeled as carbon atoms with the same Lennard-Jones parameters as those for the nanopore. Temperatures of the RTILs and the carbon nanotube atoms were maintained at 400 K . Electrostatic interactions were calculated using the PME method, and the neighbor list was updated every 2 fs . Each simulation consisted of a trial run of 5 ns to reach a steady state and a production run of 25 ns . Five independent cases were studied to estimate the error bars. To determine the ionic currents, we used the method detailed in ref 26. This requires computing the displacement of the effective charge center of the entire system $DC_c(t) = \langle 1/L_x \sum_{i=1}^N q_i [x_i(t) - x_i(0)] \rangle$, where q_i and $x_i(t \text{ or } 0)$ are the charge and x position of each atom i inside the system and $\langle \dots \rangle$ denotes the ensemble average. Next, the ionic current was obtained through a linear regression of $DC_c(t)$. Additional

simulations based on the dual-nanopore and dual-reservoir method, in which electrostatic potentials in the entire system follow Poisson's equation in a straightforward manner, were performed to ascertain that the ionic transport phenomena observed in the above simulations are independent of the way the voltage drop is applied. These simulations and other details of MD methods are documented in the Supporting Information.

■ ASSOCIATED CONTENT

● Supporting Information

MD simulation parameters and method for calculating conductivity of bulk RTILs and RTILs confined in periodic nanopores, distribution of electrical potential inside selected systems, discussion of different sensitivity of ionic conductivity on ion density between ions in nanopore and in bulk, discussions on nonlinear ionic transport in very wide pores, and details of the dual-nanopore and dual-reservoir simulations. This material is available free of charge via the Internet at <http://pubs.acs.org>.

■ AUTHOR INFORMATION

Corresponding Author

*E-mail: rqiiao@clemson.edu.

Notes

The authors declare no competing financial interest.

■ ACKNOWLEDGMENTS

We thank the Clemson-CCIT office for providing computer time. The Clemson authors acknowledge support from NSF under Grant No. CBET-1264578. R.Q. was partially supported by an appointment to the HERF program for faculty at the Oak Ridge National Laboratory (ORNL) administered by ORISE. The authors at ORNL acknowledge the support from the Center for Nanophase Materials Sciences, which is sponsored at ORNL by the Office of Basic Energy Sciences, U.S. Department of Energy.

■ REFERENCES

- Heng, J. B.; Aksimentiev, A.; Ho, C.; Marks, P.; Grinkova, Y. V.; Sligar, S.; Schulten, K.; Timp, G. Stretching DNA Using the Electric Field in a Synthetic Nanopore. *Nano Lett.* **2005**, *5*, 1883–1888.
- Simon, P.; Gogotsi, Y. Materials for Electrochemical Capacitors. *Nat. Mater.* **2008**, *7*, 845–854.
- Duan, C. H.; Majumdar, A. Anomalous Ion Transport in 2-nm Hydrophilic Nanochannels. *Nat. Nanotechnol.* **2010**, *5*, 848–852.
- Karnik, R.; Duan, C. H.; Castellino, K.; Daiguji, H.; Majumdar, A. Rectification of Ionic Current in a Nanofluidic Diode. *Nano Lett.* **2007**, *7*, 547–551.
- Shirono, K.; Tatsumi, N.; Daiguji, H. Molecular Simulation of Ion Transport in Silica Nanopores. *J. Phys. Chem. B* **2009**, *113*, 1041–1047.
- Daiguji, H. Ion Transport in Nanofluidic Channels. *Chem. Soc. Rev.* **2010**, *39*, 901–911.
- Vlassioux, I.; Smirnov, S.; Siwy, Z. Nanofluidic Ionic Diodes. Comparison of Analytical and Numerical Solutions. *ACS Nano* **2008**, *2*, 1589–1602.
- Vlassioux, I.; Siwy, Z. S. Nanofluidic diode. *Nano Lett.* **2007**, *7*, 552–556.
- Siwy, Z. S. Ion Current Rectification in Nanopores and Nanotubes with Broken Symmetry Revisited. *Adv. Funct. Mater.* **2006**, *16*, 735–746.
- Cruz-Chu, E. R.; Aksimentiev, A.; Schulten, K. Ionic Current Rectification through Silica Nanopores. *J. Phys. Chem. C* **2009**, *113*, 1850–1862.
- Dzubiella, J.; Hansen, J. P. Electric-field-controlled Water and Ion Permeation of a Hydrophobic Nanopore. *J. Chem. Phys.* **2005**, *122*, 234706.
- Dzubiella, J.; Allen, R. J.; Hansen, J. P. Electric field-controlled Water Permeation Coupled to Ion Transport Through a Nanopore. *J. Chem. Phys.* **2004**, *120*, 5001–5004.
- Powell, M. R.; Cleary, L.; Davenport, M.; Shea, K. J.; Siwy, Z. S. Electric-Field-Induced Wetting and Dewetting in Single Hydrophobic Nanopores. *Nat. Nanotechnol.* **2011**, *6*, 798–802.
- Wang, D.; Kvetny, M.; Liu, J.; Brown, W.; Li, Y.; Wang, G. Transmembrane Potential across Single Conical Nanopores and Resulting Memristive and Memcapacitive Ion Transport. *J. Am. Chem. Soc.* **2012**, *134*, 3651–3654.
- Dydek, V.; Zaltzman, B.; Rubinstein, I.; Deng, D. S.; Mani, A.; Bazant, M. Z. Overlimiting Current in a Microchannel. *Phys. Rev. Lett.* **2011**, *107*, 118301.
- Ohno, H., Ed. *Electrochemical Aspects of Ionic Liquids*; John Wiley and Sons, Inc.: New York, 2005.
- Largeot, C.; Portet, C.; Chmiola, J.; Taberna, P.-L.; Gogotsi, Y.; Simon, P. Relation between the Ion Size and Pore Size for an Electric Double-Layer Capacitor. *J. Am. Chem. Soc.* **2008**, *130*, 2730–2731.
- Lin, R. Y.; Taberna, P. L.; Fantini, S.; Presser, V.; Perez, C. R.; Malbosc, F.; Rupesinghe, N. L.; Teo, K. B. K.; Gogotsi, Y.; Simon, P. Capacitive Energy Storage from –50 to 100 °C Using an Ionic Liquid. *J. Phys. Chem. Lett.* **2011**, *2*, 2396–2401.
- Merlet, C.; Rotenberg, B.; Madden, P. A.; Taberna, P.-L.; Simon, P.; Gogotsi, Y.; Salanne, M. On the Molecular Origin of Supercapacitance in Nanoporous Carbon Electrodes. *Nat. Mater.* **2012**, *11*, 306–310.
- Rajput, N. N.; Monk, J.; Hung, F. R. Structure and Dynamics of An Ionic Liquid Confined inside A Charged Slit Graphitic Nanopore. *J. Phys. Chem. C* **2012**, *116*, 14504–14513.
- Iacob, C.; Sangoro, J. R.; Kipnusu, W. K.; Valiullin, R.; Karger, J.; Kremer, F. Enhanced Charge Transport in Nano-confined Ionic Liquids. *Soft Matter* **2012**, *8*, 289–293.
- Rajput, N. N.; Monk, J.; Singh, R.; Hung, F. R. On the Influence of Pore Size and Pore Loading on Structural and Dynamical Heterogeneities of An Ionic Liquid Confined in A Slit Nanopore. *J. Phys. Chem. C* **2012**, *116*, 5169–5181.
- Singh, R.; Monk, J.; Hung, F. R. Heterogeneity in the Dynamics of the Ionic Liquid [BMIM⁺][PF₆[–]] Confined in A Slit Nanopore. *J. Phys. Chem. C* **2011**, *115*, 16544–16554.
- Davenport, M.; Rodriguez, A.; Shea, K. J.; Siwy, Z. S. Squeezing Ionic Liquids through Nanopores. *Nano Lett.* **2009**, *9*, 2125–2128.
- Karnik, R.; Fan, R.; Yue, M.; Li, D. Y.; Yang, P. D.; Majumdar, A. Electrostatic Control of Ions and Molecules in Nanofluidic Transistors. *Nano Lett.* **2005**, *5*, 943–948.
- Aksimentiev, A.; Schulten, K. Imaging α -Hemolysin with Molecular Dynamics: Ionic Conductance, Osmotic Permeability, and the Electrostatic Potential Map. *Biophys. J.* **2005**, *88*, 3745–3761.
- Roux, B. The Membrane Potential and its Representation by a Constant Electric Field in Computer Simulations. *Biophys. J.* **2008**, *95*, 4205–4216.
- Shim, Y.; Kim, H. J. Nanoporous Carbon Supercapacitors in an Ionic Liquid: A Computer Simulation Study. *ACS Nano* **2010**, *4*, 2345–2355.
- Merlet, C.; Péan, C.; Rotenberg, B.; Madden, P. A.; Simon, P.; Salanne, M. Simulating Supercapacitors: Can We Model Electrodes As Constant Charge Surfaces? *J. Phys. Chem. Lett.* **2013**, *4*, 264–268.
- Daily, J. W.; Micci, M. M. Ionic Velocities in An Ionic Liquid under High Electric Fields Using All-atom and Coarse-grained Force Field Molecular Dynamics. *J. Chem. Phys.* **2009**, *131*, 094501.
- Qiao, R.; Aluru, N. R. Atypical Dependence of Electroosmotic Transport on Surface Charge in a Single-wall Carbon Nanotube. *Nano Lett.* **2003**, *3*, 1013–1017.
- Qiao, R.; Aluru, N. R. Surface-Charge-Induced Asymmetric Electrokinetic Transport in Confined Silicon Nanochannels. *Appl. Phys. Lett.* **2005**, *86*, 143105.

- (33) Keskin, S.; Kayrak-Talay, D.; Akman, U.; Hortacsu, O. A Review of Ionic Liquids towards Supercritical Fluid Applications. *J. Supercrit. Fluids* **2007**, *43*, 150–180.
- (34) Hess, B.; Kutzner, C.; van der Spoel, D.; Lindahl, E. GROMACS 4: Algorithms for Highly Efficient, Load-Balanced, and Scalable Molecular Simulation. *J. Chem. Theory Comput.* **2008**, *4*, 435–447.
- (35) Roy, D.; Maroncelli, M. An Improved 4-Site Ionic Liquid Model. *J. Phys. Chem. B* **2010**, *114*, 12629–12631.
- (36) Alexiadis, A.; Kassinos, S. Molecular Simulation of Water in Carbon Nanotubes. *Chem. Rev.* **2008**, *108*, 5014–5034.